Available online at www.sciencedirect.com

ScienceDirect

Procedia Engineering 81 (2014) 1283 – 1287

Procedia Engineering

www.elsevier.com/locate/procedia

11th International Conference on Technology of Plasticity, ICTP 2014, 19-24 October 2014, Nagoya Congress Center, Nagoya, Japan

Influence of pearlite interlamellar spacing on strain hardening behaviour in spring steel 60Si2MnA

Chao-lei Zhang*, Xiang Liu, Le-yu Zhou, Ya-zheng Liu

School of Materials Science and Engineering, University of Science and Technology Beijing, Beijing, 100083, China

Abstract

Influence of the pearlite interlamellar spacing on the strain hardening behavior with systematically various pearlite fineness (within the range 140 to 510 nm) obtained by isothermal transformation has been investigated in spring steel 60Si2MnA. Based on the uniaxial tensile tests carried out at ambient temperature, an empirical relationship between the measured strain hardening exponent and interlamellar spacing was found.

Selection and peer-review under responsibility of the Department of Materials Science and Engineering, Nagoya University

Keywords: Pearlitic steel; Spring steel; Interlamellar spacing; Strain hardening

1. Introduction

Pearlite is the base or a substantial structure constituent of many high strength steels. As one of them, spring steel 60Si2MnA is often hard drawn into a wire and then coiled into springs by hot deformation, or increasingly directly manufactured into springs by cold deformation (Ai et al., 2003; Ai et al., 2005). The required microstructure of the steel is the thin interlamellar spacing, small pearlite colony and less free ferrite bulk volume. In spite of the relatively simple microstructure of pearlite and many studies of its properties, strain hardening is far from being understood.

* Corresponding author. Tel.: +86-10-62333174 ; fax: +86-10-6239-6861
E-mail address: zhangchaolei@ustb.edu.cn

Selection and peer-review under responsibility of the Department of Materials Science and Engineering, Nagoya University
doi:10.1016/j.proeng.2014.10.111

The empirical equations used to describe experimental stress-strain curve summarizes has been summarized and compared by several investigators (Kleemola et al., 1974; Umemoto et al., 2000). The Hollomon (1945) analysis is the most commonly used empirical analysis method, as showing in Eq. (1).

$$S = \mathrm{C} \cdot e^{\mathrm{n}} , \tag{1}$$

where S is the true stress, e is the true plastic strain, C is a parameter of the material and n is the strain hardening exponent. And there is an empirical Hall-Petch type equation as showing in Eq. (2) which relates flow stress with interlamellar spacing in the nearly fully pearlitic structure steels (Modi et al., 2001; Hyzak et al., 1976; Elwazri et al., 2005).

$$\sigma_i = \sigma_0 + \mathrm{k} \cdot S_{\mathrm{p}}^{-\mathrm{m}} , \tag{2}$$

where σ_{j} is the yield or ultimate stress, σ_{o} is the friction stress, S_{P} is the interlamellar spacing, m and k is the material constant. Hence, there is an implied correlation between the strain hardening exponent in Eq. (1) and the interlamellar spacing in Eq. (2).

In fact, a number of work has been devoted to the strain hardening behaviour in low carbon steels to date (Antoine et al., 2006; Deva et al., 2011; Morrison, 1966), and an empirical relationship between the strain hardening exponent (n) and ferrite grain size (d, mm) has been established by Morrison (1966) as Eq. (3).

$$n = \frac{5}{10 + 1/\sqrt{d}} . \tag{3}$$

However, no relationship between the interlamellar spacing and strain hardening exponent was established. The work described in this paper is a study of the effects of pearlite fineness on the strain hardening behavior in spring steel 60Si2MnA during tensile deformation process.

Nomenclature

C	a parameter of the material
D_{A}	prior-austenization grain size
d	ferrite grain size
e	true plastic strain
j	represent the yield or ultimate stress
k	a material constant
m	a material constant
n	strain hardening exponent
S	true stress
S_{P}	interlamellar spacing
ε	engineering strain
σ	engineering stress
σ_{j}	yield or ultimate stress
σ_{o}	friction stress

2. Experimental procedure

The spring steel used in this work had a chemical composition of 0.60%C-0.75%Mn-1.69%Si-0.14%Cr-0.011%P-0.008%S (in wt%). Two-step heat treatments given in Table 1 were carried out to produce a systematic variation in microstructure. Here specimens were austenitized at 950 °C for 30 min to permit full austenitization. After austenitizing, the specimens were quenched into a salt pot for isothermal transformation of the austenite

phase at temperatures at intervals of 30 °C from 570 to 660 °C. Transformation times were chosen sufficient to ensure complete transformations, without appreciable spheroidization. All the specimens after the heat treatments were metallographically polished and then etched with 4% nital for microstructural observation by optical microscope. Then, interlamellar spacing and pearlitic colony size were measured by random intercept methods. Besides, tensile test was carried out on a WAW-200 testing machine at a crosshead speed of 10 mm/min at ambient temperature in air and using standard specimens (gauge diameter 5 mm, gauge length 25 mm).

Table 1. Two-step heat treatments schedule.

Exp. No.	1	2#	3#	4#
Austenization temperature, (°C)	950	950	950	950
Salt bath temperature (°C)	570	600	630	660

3. Results and discussion

The optical micrographs showing the microstructure of the steel samples 1-4# are given in Fig. 1. The microstructure examination revealed the presence of plenty of pearlite, and a small quantity of free ferrite which proceeds along the prior-austenite grain boundaries. As expected, the prior-austenite grain size was kept constant due to the constant austenitization temperature, but the interlamellar spacing was increasing with increased the isothermal transformation temperature. The quantitative metallographic of the two microstructure characteristics in the samples 1-4# are tabulated in Table 2.

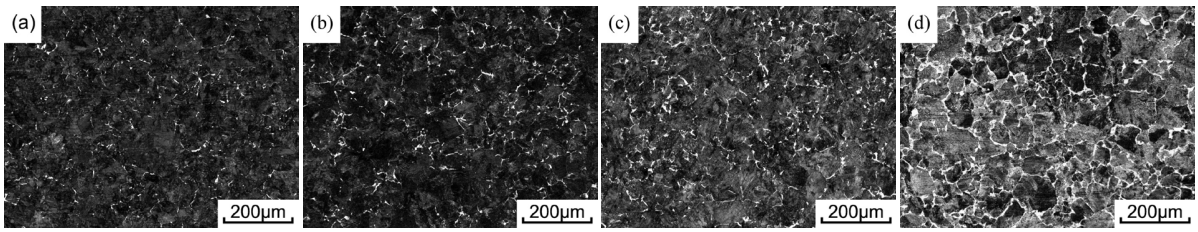

Fig. 1. Optical micrographs showing microstructure: (a) 1#; (b) 2#; (c) 3#; (d) 4#.

The engineering stress-engineering strain curves of the steels samples 1-4# are plotted in Fig. 2. As can be seen from the shape of the curves from 1# to 4#, the yield and ultimate tensile strength decrease progressively, and the uniform elongation becomes larger while the local elongation in the neck becomes smaller. As is known, the fine pearlite is higher strength and more ductile than the coarse one. Consequently, the main reason for this is that the interlamellar spacing increases progressively (140, 190, 280, and 510 nm from 1# to 4# tabulated in Table 2).

Table 2. Quantitative metallographic and strain hardening exponent of steel samples 1-4#.

Exp. No.	Interlamellar spacing S_P(nm)	prior-austenization grain size D_A (μm)	Strain hardening exponent n
1#	140	60	0.27
2#	190	60	0.30
3#	280	60	0.31
4#	510	60	0.32

Eq. (4) as given below is derived on taking logarithm on both left hand and right hand sides of Eq. (1). A linear relationship exists between log S and log e. Then, the coefficients, n and C, can be calculated from the slope and intercept of the log S - log e curve, respectively.

$$\log S = \log \mathrm{C} + \mathrm{n} \cdot \log e \quad . \tag{4}$$

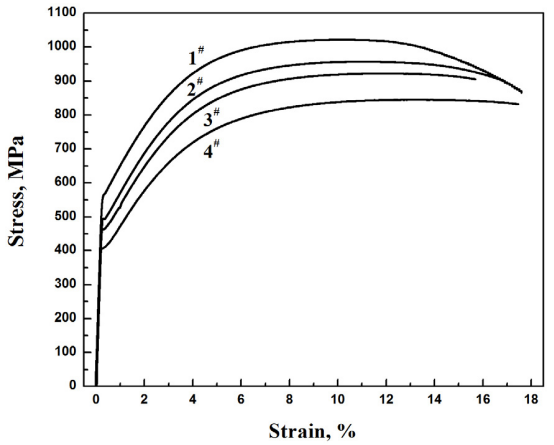

Fig. 2. Engineering stress-engineering strain curves of steel samples 1-4#.

And the true stress-engineering stress (σ) and true strain-engineering strain (ε) relations exist as Eqs. (5) and (6), respectively. As a result, the true stress and true strain can be calculated from the engineering stress-engineering strain curves (Fig. 2).

$$S = (1+\varepsilon)\cdot\sigma \tag{5}$$

$$e = \ln(1+\varepsilon)\ . \tag{6}$$

The log S - log e curves of the steel samples 1-4# are plotted in Fig. 3(a). The linear relationship described by linear curve fitting exists between log S and log e, and Eq. (4) is obeyed over the full range of uniform strain. A complete list of the strain hardening exponent is contained in Table 2.

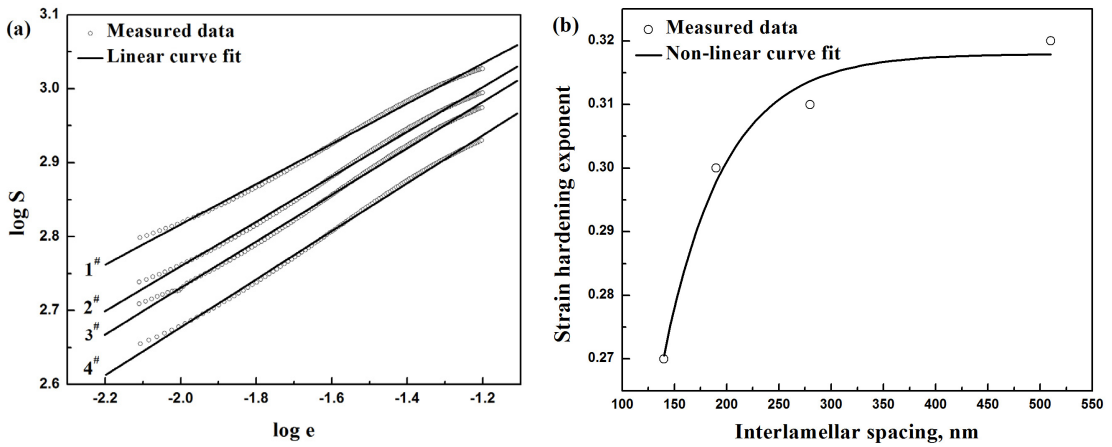

Fig. 3. (a) log S - log e curves and (b) relation of interlamellar spacing to the strain hardening exponent.

Obviously, for the spring steel 60Si2MnA, the microstructure of which is a typical hypoeutectoid, all three microstructural features, the interlamelar spacing, pearlitic colony size and volume fraction of free ferrite have an impact on the mechanical properties. However, in high-carbon ferrite-pearlite steels, interlamellar spacing is the determining factor of the mechanical properties (Hyzak et al., 1976; Elwazri et al., 2005). In order to evaluate the

effect of the pearlite fineness on the strain hardening behavior, the strain hardening exponent has been plotted against the interlamellar spacing in Fig. 3(b). It can be seen that the strain hardening exponent is increased sharply with an increase in the interlamellar spacing from 140 to 280 nm. However, with a further increase in the interlamellar spacing to 510 nm, the strain hardening exponent values increase marginally. With the increasing of the interlamellar spacing, the size of ferrite lamellae becomes lager. Then, the steel can have lager degree of deformation strengthening. That is means the strain hardening exponent gradually increased. The following approximate relationship between S_P (nm) and n described by non-linear curve fit as Eq. (7) was found for the spring steel.

$$n = -0.52 \cdot \exp\left(-\frac{S_p}{58.29}\right) + 0.32 \ . \tag{7}$$

4. Conclusions

The strain hardening exponent increases sharply with the increase in interlamellar spacing up to a critical value (280 nm), above which further increases in the interlamellar spacing result in no substantial increase in the strain hardening exponent. For the spring steel 60Si2MnA, an empirical correlation between the interlamellar spacing and strain hardening exponent were determined as $n = -0.52 \cdot \exp(-S_P/58.29)+0.32$.

References

Ai, J.H., Zhao T.C., Gao H.J., Hu Y.H., Xie X.S., 2005. Effect of controlled rolling and cooling on the microstructure and mechanical properties of 60Si2MnA spring steel rod. Journal of Materials Processing Technology, 160 (3), 390-395.

Ai J.H., Xu J., Gao H.J., Hu Y.H., Xie X.S., 2003. Artificial neural network prediction of the microstructure of 60Si2MnA rod based on its controlled rolling and cooling process parameters. Materials Science and Engineering A, 344 (1-2), 318-322.

Kleemola H.J., Nieminen M.A., 1974. On the strain-hardening parameters of metals. Metallurgical and Materials Transactions B, 5 (8), 1863-1866.

Umemoto M., Liu Z.G., Sugimoto S., Tsuchiya K., 2000. Tensile stress-strain analysis of single-structure steels. Metallurgical and Materials Transactions A, 31 (7), 1785-1794.

Hollomon J.H., 1945. Tensile deformation. Transactions of the Metallurgical Society of AIME, 162, 268-290.

Modi O.P., Deshmukh N., Mondal D.P., Jha A.K., Yegneswaran A.H., Khaira H.K., 2001. Effect of interlamellar spacing on the mechanical properties of 0.65% C steel. Materials Characterization, 46 (5), 347-352.

Hyzak J.M., Bernstein I.M., 1976. The role of microstructure on the strength and toughness of fully pearlitic steels. Metallurgical and Materials Transactions A, 7 (8), 1217-1224.

Elwazri A.M., Wanjara P., Yue S., 2005. The effect of microstructural characteristics of pearlite on the mechanical properties of hypereutectoid steel. Materials Science and Engineering A; 404 (1-2), 91-98.

Antoine P., Vandeputte S., Vogt J.B., 2006. Empirical model predicting the value of the strain-hardening exponent of a Ti-IF steel grade. Materials Science and Engineering A, 433 (1-2), 55-63.

Deva A., Jha B.K., Mishra N.S., 2011. Influence of boron on strain hardening behavior and ductility of low carbon hot rolled steel. Materials Science and Engineering A, 528 (24), 7375-7380.

Morrison W.B., 1966. The effect of grain size on the stress-strain relationship in low-carbon steel. ASM Transactions Quarterly, 59 (4), 824-846.